Contract No.:

This manuscript has been authored by Battelle Savannah River Alliance (BSRA), LLC under Contract No. 89303321CEM000080 with the U.S. Department of Energy (DOE) Office of Environmental Management (EM).

ENGINEERED NANO-ANTENNA SUSCEPTOR AS EFFICIENT PLATFORMS FOR EFFICIENT UPTAKE AND RELEASE OF ANALYTES

Simona E. Hunyadi Murph*[1,2] Sarah Schyck,[1] and Kaitlin Lawrence[1]

[1] **Savannah River National Laboratory**
Aiken, South Carolina, USA

[2] **University of Georgia**
Athens, Georgia, USA

*Corresponding author: E-Mail: Simona.Murph@srnl.doe.gov, Phone: 803-646-6761

Abstract

An efficient and rapid technique has been developed to enhance detection and extraction of organic dye contaminants from aqueous media using iron oxide-based nanomaterials. The technology is used to remotely remediate environments by scavenging and removing species from water sources at desired location. An electromagnetic field is selectively coupled to engineered iron oxide-based nano-antenna susceptor for nanoparticles's regeneration and reuse. Specifically, the adsorption and removal of a model analyte, methylene blue dye (MB) identified here as 'payload', from a simulated contaminated water media is demonstrated. Remote manipulation of 'payloads' adsorbed on iron oxide-based materials is achieved through a non-contact and highly selective thermal process. Heat is selectively generated through susceptor nano-antennas, i.e. iron oxide-based nanomaterials, when exposed to an electromagnetic field. The release of 'payload' from the iron oxide nanoparticles is due to localized temperature increase in the surrounding media upon exposure to the electromagnetic field. Heating is localized and occurs extremely fast, reducing the wasted thermal load on the environment. The susceptor nano-antennas can be activated remotely to generate localized heat on demand. Careful selection of the nano-antenna's composition and surface chemistry permits manipulation and control of the adsorption and regeneration thermal process. Contaminant dye removal via adsorption onto sorbent media is faster, easier, and more economic and is therefore, the industrially preferred.

Keywords: nano-antennas, electromagnetic field, iron-oxide nanomaterials, susceptors, environmental stewardship, localized heating.

1. Introduction

Magnetic nanomaterials, which are typically viewed as materials responsive to an applied magnetic field, have been used for years for gas manipulation [1, 2], sensing [3, 4], magnetic resonance imaging [5], photothermal applications [6], biotherapy [7], and water treatment [8] applications. This is due to their unique properties including high surface area, high adsorption efficiency, enhanced reactivity, low cost, rapid collection due to their magnetic characteristics, and low environmental impact [9,10]. Magnetic nanoparticles, however, often undergo agglomeration and aggregation without appropriate protection or passivation of their surfaces. Therefore, nanomaterial's surface is often manipulated and engineered with a variety of capping ligands, stabilizers, or polymers through physisorption of chemisorption processes. The selection of the surface ligands influences the nanomaterial's physicochemical properties of the surface, such as reactivity, stability, hydrophilicity/hydrophobicity, surface charge and dispersibility in media [9-12]. These characteristics further influence and controls nanoparticle's behavior and use for targeted applications. Magnetic nanostructures are often coupled with nanomaterials with dissimilar properties, such as noble metals, to create novel hybrid nanostructures with improved properties [13].

Iron oxides are abundant in nature and have been used in applications such as information storage fields, magnetic sensors, magnetic refrigeration, ferrofluids, hyperthermia bio-medical applications, and separations [14, 15]. The most common iron oxide material used in these applications uses magnetite Fe_3O_4, maghemite, γ-Fe_2O_3, and hematite α-Fe_2O_3. We reported earlier the use of iron oxide (Fe_2O_3) for controlled release and separation of hydrogen isotopes [1, 16]. For example, protium and deuterium were rapidly desorbed from magnetic-hydride iron oxide-palladium (iron oxide-palladium) nanomaterials using an electromagnetic field. The magnetic-hydride nanomaterial susceptors serve as a local nano-antenna that absorb electromagnetic energy. Subsequently, the energy is released as heat in the surrounding media by hysteresis loss or relaxation mechanisms leading to the selective and methodical release of hydrogen isotopes.

Organic dyes are often inadvertently released into the wastewater as byproducts of manufacturing of various products including textiles and pharmaceuticals [17-19]. These contaminant organic dyes are persistent in the environment and breakdown into products that are toxic, mutagenic or carcinogenic [20]. As a result, a viable technology is needed to selectively scavenge these species and remove them from water sources. Magnetic nanoparticles, e. g. Fe_2O_3, are efficient sorbent materials for environmental remediation processes [8]. The adsorption process is highly dependent on the environment's pH, organic dye concentration, temperature, time, surface interactions, among others. Bare magnetic iron oxide nanoparticles can be used for organic dye removal; however, it was found that surface functionalization with chemical moieties can improve the adsorption efficiency while increasing their dispersibility. For example, adsorption of organic dyes, including cationic (methylene blue, MB) or anionic (methyl orange, MO) dyes on magnetic iron oxide nanoparticles was reported [17-19]. However, adsorption is not fully reversible versus the pH or ionic strength change likely because of a weak contribution of non-electrostatic interactions. Magnetic Fe_3O_4@C nanoparticles were also employed as adsorbents for removal of organic dyes from aqueous solution [21]. Methyl violet dye was successfully removed from wastewater sample with iron oxide modified with sodium dodecyl sulfate (SDS) as an anionic surfactant. While the adsorption process is reversible in this case, unfortunately, the process requires the use of pollutant organic solvents to regenerate the nanoparticle's surface. The process is therefore cumbersome and requires multiple purification steps. Therefore, cost effective and non-polluting materials and sequestration technologies that can be easily deployed in contaminated areas are needed. Moreover, these technologies should allow efficient retrieval and disposal of contaminants in a safe manner and does not generate additional waste. Nanomaterials can be used as efficient sorbent materials of contaminants because they have an increased surface area-to-volume ratio and show higher reactivity than bulk [22]. Nanoparticle's surface chemistry can be easily tailored for targeted in situ sensing and remediation processes.

In this research study, organic dyes were adsorbed onto bare and surface-engineered magnetic nanoparticles, i. e. citrate and cetyltrimethylammonium bromide, and then remotely desorbed using an alternating magnetic field. Iron oxide nanoparticles were also modified with gold nanoparticles through a simple metal ion reduction approach. The effect of concentration and metal domain growth on magnetic hyperthermia was investigated. An electromagnetic field was selectively coupled to engineered iron oxide-based nano-antenna susceptor for the adsorption and removal of a model analyte, methylene blue dye (MB) identified here as 'payload', from a simulated contaminated water media.

2. Materials and Instrumentation

Chloroauric acid ($HAuCl_4$), sodium citrate (>99%), cetyltrimethylammonium bromide (CTAB), and methylene blue were purchased from *Sigma Aldrich*. All aqueous solutions were prepared in deionized water. All glassware used in the following protocols was cleaned with Aqua Regia and then rinsed with deionized water. A *Fischer Scientific* accuSpin Micro17R was used for centrifuging the nanoparticles. A *TECS USA* MCS PDA with LS ultraviolet–visible was used to evaluate nanoparticle's optical properties. The Zeta sizer and Zeta potential of the nanoparticles were obtained using a *Brookhaven Instruments* DLS NanoBrook Omni (110-240 V) manufactured in 2014. A *Hitachi* SU8200 Scanning Electron Microscope coupled with energy dispersive X-Ray spectroscopy was used for evaluating nanomaterials morphologies and compositions.

3. Experimental Section

3.1. Iron oxide surface functionalization with sodium citrate or cetyltrimethylammonium bromide (CTAB)

Bare iron oxide (Fe_2O_3) nanoparticles were incubated in 1% sodium citrate or 0.1 M cetyltrimethylammonium bromide (CTAB) for up to 24 hrs. Subsequently, nanoparticles were washed with deionized water and magnetically separated with a neodymium magnet.

3.2. Iron oxide-gold nanoparticles (Fe_2O_3-Au)

To prepare iron oxide-gold hybrid nanostructures, gold was reduced in the presence of iron oxide nanoparticles using the Turkevich method [10]. To accomplish this, 10 mL water with 0.1 mL of 25 mM iron oxide (Fe_2O_3) and 1 mL of 1% trisodium citrate was boiled before 0.25 mL of 0.01 M chloroauric acid ($HAuCl_4$) was added. Once the solution turned ruby red, it was cooled and magnetically purified three times using a rare earth magnet. To adjust gold nanoparticle size, the amount of trisodium citrate was varied by 2, 3, 3.5, 4, 4.5, 5, and 10 mL while 0.25 mL of 0.01 M chloroauric acid ($HAuCl_4$) was held constant. The final purified iron oxide-gold conjugates were suspended in water.

3.2. Iron oxide-based nanoparticles adsorption and release or organic dyes

Iron oxide-based nanoparticles, i. e. bare, citrate functionalize and cetyltrimethylammonium bromide (CTAB) functionalized, were incubated in methylene blue (MB) dye. Batch adsorption experiments were carried out at room temperature. The adsorption of methylene blue solution was measured by examining the in-situ ultraviolet–visible transmission spectra of the methylene blue solution using an Ocean Optics spectrophotometer (USB 2000). The absorbance peak at λ = 664 nm was monitored at regular time increments of 20 min and were used to evaluate the adsorption rate of methylene blue. Electromagnetic

field was generated using a 10.0 kW magnetic induction system (Magnetic Hyperthermia System, MSI Automation, Inc., Wichita, KS) designed to operate between 250 and 450 kHz and equipped with a 425 kHz resonance frequency water cooled copper coil (6 turns, 17.5 mm radius, and 47.5 mm height). Electromagnetic field densities of 10−60 kA/m could be generated depending upon the power setting as well as the size and shape of the heating coil.

4. Results and Discussion

4.1. Surface engineering of iron-oxide based nanostructures

Bare iron oxide (Fe_2O_3) nano-spherical materials were characterized using scanning electron microscopy (SEM). Data shows (Figure 1 a) that the spherical nanomaterials have an outer diameter of 46 ± 5 nm. Subsequently, the surface of bare iron oxide nano-spherical materials was engineered with different capping agents and further explored as a sorbent platform. Two different capping ligands specifically sodium citrate and cetyltrimethylammonium bromide (CTAB) were selected in this study to engineer the surface of iron oxide nano-spherical materials. The chemical structure of the moieties used are displayed in figure 1 b and c.

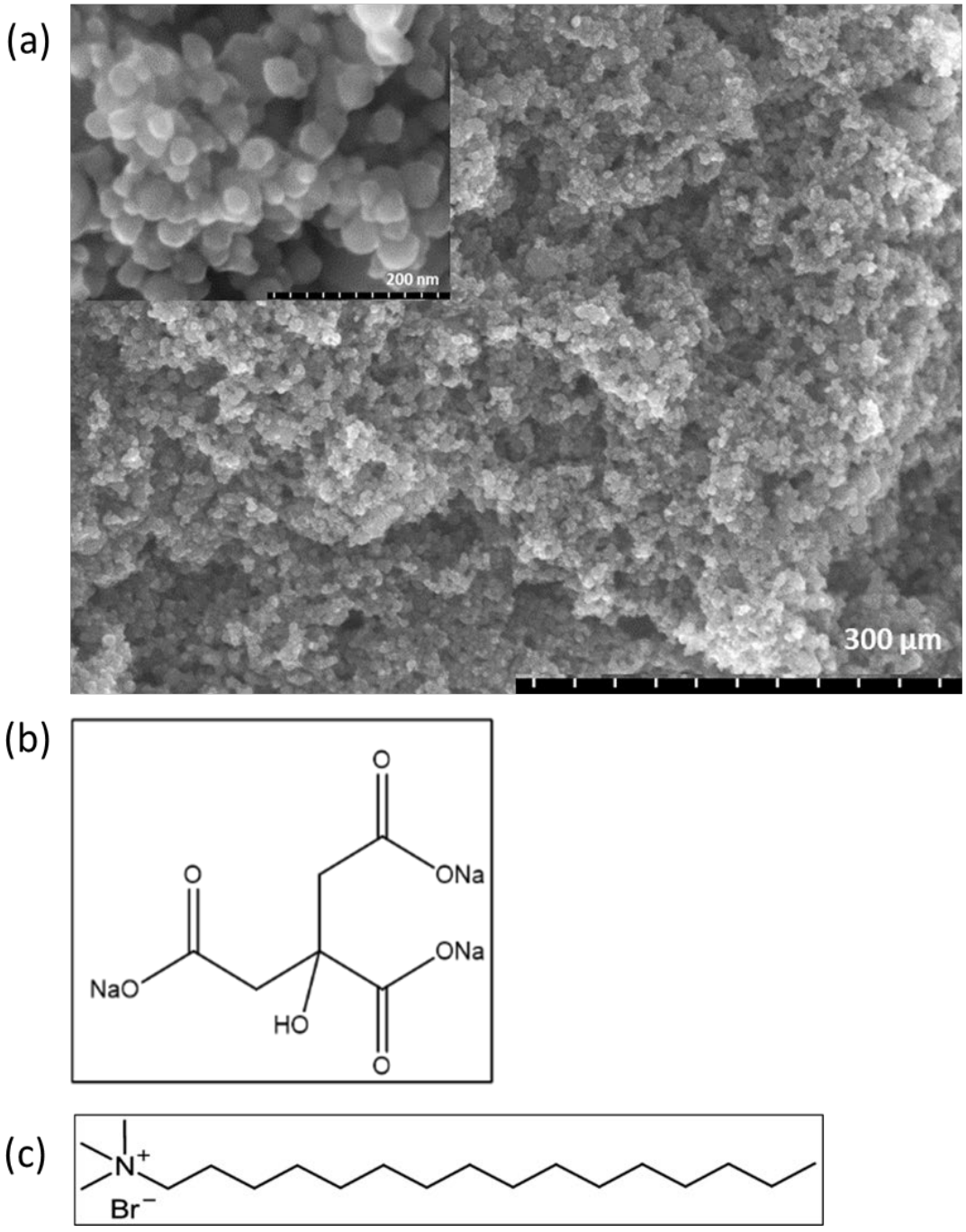

Figure 1. (a) Scanning electron microscopy images of bare iron oxide nanoparticles. Chemical structure of (a) sodium citrate and (b) cetyltrimethylammonium bromide (CTAB).

The dynamic properties of the nanoparticles in solution are important tools to evaluate nanoparticle behavior in relevant solution-based environments. The zeta (ζ) potential was measured for each sample to evaluate and confirm the surface engineering charge modification. As shown in Table 1, the zeta potential values decreased for the citrate engineered particles and increased for the cetyltrimethylammonium bromide

modified particles. The effective surface charge of the bare iron oxide in deionized water was negative with a value of −16 mV. The negative surface charge is attributed to the electric potential formed at the solid support−liquid interface due to the presence of hydroxide ions adsorbed on the surface, specifically the deprotonated −Fe−OH species [10, 23]. Once their surface was engineered, the surface charge fluctuated depending on the capping agent used. For example, citrate functionalization renders a negative surface charge. The initial negative surface charge of -16 mV became more negative, reaching values of – 24mV. The citrate adsorption on the iron oxide nanoparticles is achieved by the coordination of carboxylate functionalities of the citrate. Immersion in cetyltrimethylammonium bromide leads to a less negative surface charge of -2mV. This is predictable as an electrostatic interaction takes could occur between deprotonated −O− of the −Fe−OH species with the positive cetyltrimethylammonium bromide head group. As previously reported [1, 10], the hydrophobic tails of cetyltrimethylammonium bromide interdigitate creating a "zipper"-type bilayer on the nanoparticles' surface. Therefore, the first cationic group is electrostatically binding at the nanoparticle's surface with the deprotonated −O− species, while the second cationic head group of the zipper-like structure of the cetyltrimethylammonium bromide is exposed to the environment, rendering it a less negative surface charge. As expected, upon surface functionalization with citrate or cetyltrimethylammonium bromide moieties, no changes in the outer diameter of individual nanoparticles were observed.

Table 1. Effect of ligand exchange on zeta potential.

Sample	**ζ (mV)**
Fe_2O_3	-15.98 ± 5
Fe_2O_3-Citrate	-24.08 ± 2
Fe_2O_3-CTAB	-2.11 ± 3

4.2. Surface engineering of iron oxide nanoparticles with gold nanoparticles

Multifunctional iron oxide-gold nanomaterials have been designed and created as a way of improving and expanding the properties and applications of the bare iron oxide nanomaterial. Coupling gold with iron oxide creates nanocomposite materials with a wider range of applications. These are mostly due to the unique properties of gold nanoparticles that support localized surface plasmon resonances (LSPR) [3, 10]. Explicitly, the free electrons in the gold nanometals collectively oscillate when resonantly driven by electromagnetic radiation. These localized surface plasmon resonances can generate intense, highly confined electromagnetic fields thereby enabling the use of such nanometals in a variety of applications in catalysis, biotechnology, sensing, imaging, energy, among others [1, 3, 8, 9, 23].

Iron oxide nanospheres were engineered with gold nanoparticles through a citrate reduction approach. In this reaction, iron oxide serves as a support or nucleation center for subsequent reduction of gold ions with a reducing agent, i. e. sodium citrate. This one step simple process leads to the creation of hybrid iron oxide-gold nanostructures adorned with gold nanosphere. The size of the gold nanoparticles on the iron oxide-gold nanocomposites was tailored by altering the trisodium citrate concentrations. Gold nanoparticle's generation can be easily monitored due to their unique optical properties. For example, during the synthesis procedure, the color of the nanoparticle reaction solution varied from a bright ruby-red

color to a red-purple color as citrate concentration decreased. There is a strong correlation between the resulting size of gold nanoparticle and the concentration of the reduction agent. Typically, lower concentration of caping agent, i. e. citrate, leads to the production of larger gold nanoparticles. Figure 2 shows scanning electron microscopy images of six different gold-iron oxide nanocomposite samples produced by varying concentrations of trisodium citrate. The diameters of the gold nanoparticles were found to vary from 32±5 nm to 12±2 nm depending on the ratios between gold ions and sodium citrate (Table 2). Notable differences were observed between nanoparticle sizes created on iron oxide support in comparison with the gold nanoparticles present in the supernatant solution. Scanning electron microscopy images show that gold nanoparticle's diameter created on the iron oxide nanoparticles range from 12nm to 17nm. Specifically, samples a-d produced on iron oxide had an average gold nanoparticle size of 17±2 nm while samples e and f produced on iron oxide only had average nanoparticle size of 12±2 nm. The smaller dimension variations for gold nanospheres grown on an iron oxide support shows that the steric effects, support's facet boundaries and surface topography influence the nanoparticle's diameter.

Table 2. The average gold nanoparticle size in relation to the concentration of trisodium citrate.

Sample Identity	Trisodium Citrate (mL)	Particle Size (nm)	Standard Dev.
a	2	32	5
b	3	21	4
c	3.5	19	4
d	4	14	4
e	4.5	13	3
f	5	12	2

Typical scanning electron microscopy image are displayed below.

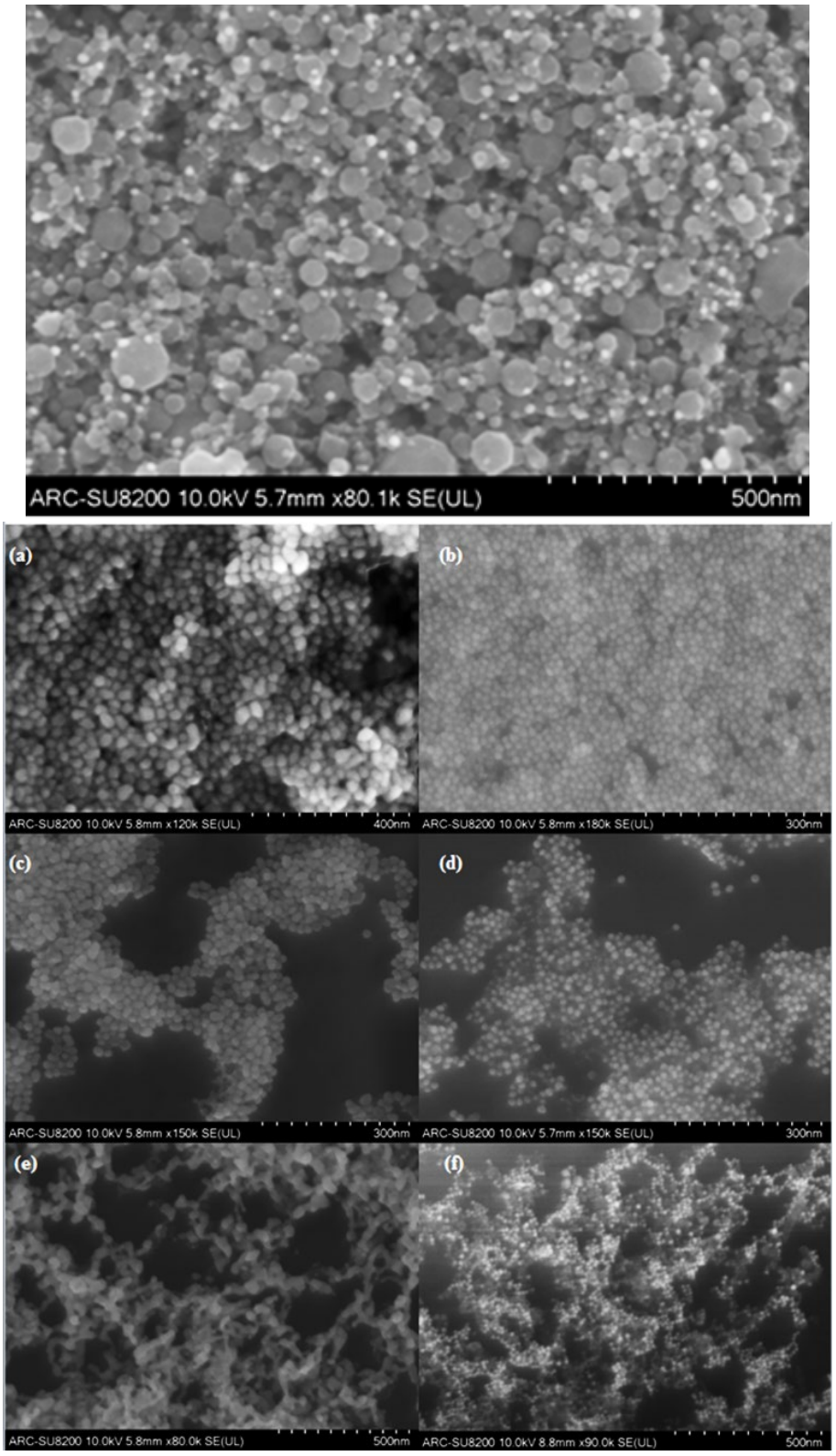

Figure 2. (top) Scanning electron microscopy images of iron oxide- gold nanostructures prepared by a sodium citrate reduction. (bottom) Scanning electron microscopy images of gold nanoparticles made from

the supernatant of gold-iron oxide nanocomposites prepared by different trisodium citrate volumes: (a) 2 mL, (b) 3 mL, (c) 3.5 mL, (d) 4 mL, (e) 4.5 mL, and (f) 5 mL.

The compositions of the different structures have been investigated by energy dispersive X-ray analysis (EDS). Data shows (Figure 3a) that the gold loading onto iron oxide nanoparticles can be tailored by simply changing the ratio between gold ions and citrate. The gold loading can be tailored from approximatively 6% to 20% loading by varying the experimental conditions. The optical properties of the nanomaterials were evaluated by ultraviolet-visible spectroscopy (Figure 3 b, c). In deionized water, the gold nanoparticles display the characteristic peak at around 520 nm that corresponds to the localized plasmon band for spherical gold nanoparticles of approximatively 15 nm. A red shift is recorded on nanoparticles larger in diameter in agreement with published research [6, 10, 12].

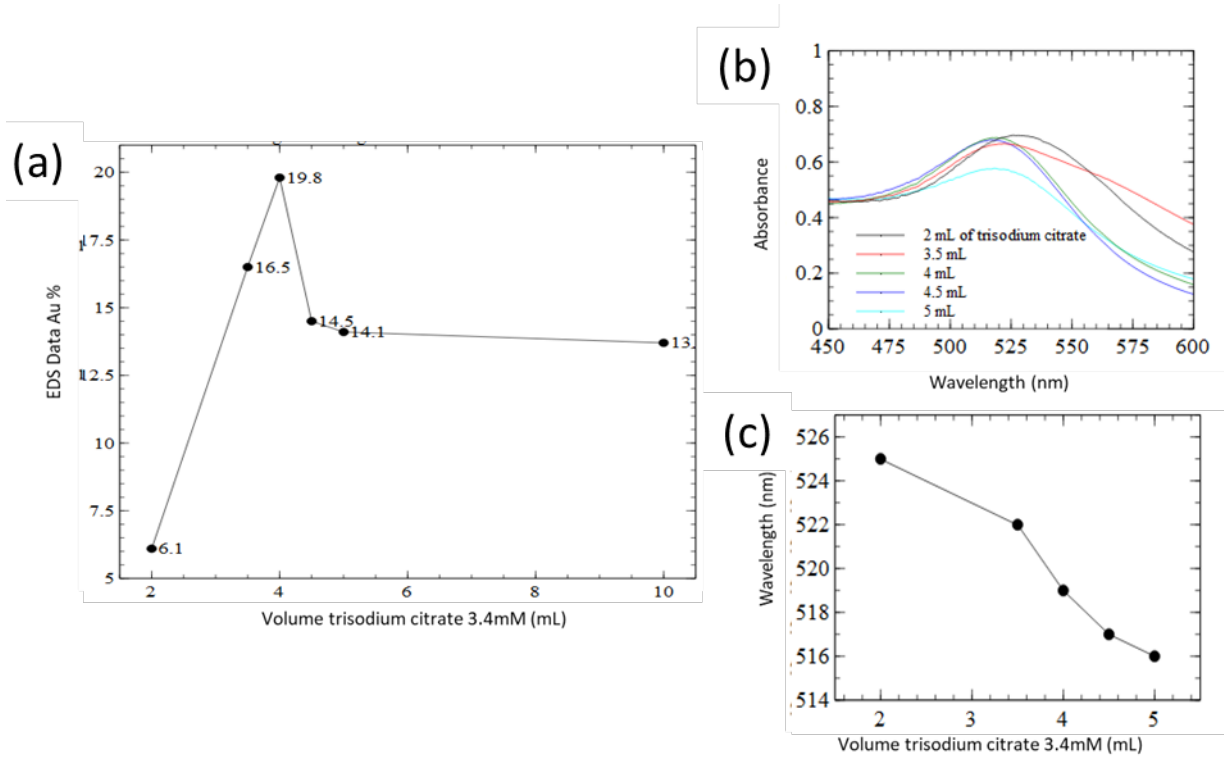

Figure 3. (a) A graph depicting the gold loading onto iron oxide dependent on the trisodium citrate amount involved in the synthesis. (b) The ultraviolet-visible absorbance of the gold nanoparticle supernatant solutions; the localized plasmon band is red shifting as the nanoparticle diameter increases. (c) Localized plasmon band peaks plotted in relation to the gold nanoparticle's size.

4.3. Magnetic induced heating of iron oxide- gold nanocomposite materials

The magnetic induced heating behavior of aqueous solutions of iron oxide and hybrid iron-oxide gold nanostructures were collected and analyzed. The susceptor antenna, defined as a material that absorbs electromagnetic energy and converts it to heat, in our case is the iron oxide nanoparticle. The heating occurs because the magnetic moment of the iron oxide nanoparticle changes direction to line up with the external field, which generate local heating [1, 24]. This change of direction can take place two different ways: Brownian relaxation, where the nanoparticle physically rotates so the moment lines up with the external

field, and Neel relaxation, where the particle is stationary, but the magnetic moment rotates in the fixed lattice [1, 24]. This is a selective process as the nano-antenna susceptors only are activated remotely and generate localized heat on demand. The heating method is non-contact and can be systematically controlled. Heating occurs extremely fast reducing the 'wasted' thermal load on the environment. Remote manipulation of 'payloads' can be achieved by strategically placing nano-antenna susceptors at desired locations. The mechanism of release is based on the temperature increase of the sorbent nanomaterial.

The magnetic induction heating efficiencies of the nanoparticles were investigated by placing the nanoparticle solutions in a magnetic field with a frequency of 425 Hz and measuring the temperature in situ, *T,* of the solution versus the field exposure time, *t.* To compare the efficiencies of the different nanoparticles, we calculate the specific loss power (SLP):

$$SLP = \frac{CVs}{m}\frac{dT}{dt}.$$

In this formula, C is the volume of specific heat capacity, $C_{water} = 4185\frac{J}{LK}$ $V_s = 12mL$ is the sample volume, and m is the mass of iron oxide. The slope of the heating curve , $\frac{dT}{dt}$, is measured using the initial rise of the heating curve. This method excludes the plateau section of the heating curve. The specific loss power values of the varying gold loading onto iron oxide nanoparticles dispersed in water are represented in Table 3.

Table 3. The calculated specific loss power (SLP) data collected on iron oxide-gold nano-antenna susceptors.

Gold Loading (%)	**Specific loss power (watts/gram)**	**Standard Deviation**
0	886	96
6	519	52
14	962	133
15	1061	155
17	929	100
20	1062	126

A dependence of heating efficiency on gold loading is observed. The calculated specific loss power increased with a higher loading of gold nanoparticles on iron oxide nanoparticles where the maximum specific loss power was 1062 at ~20% gold loading. However, data shows that heating plateaus at approximately 15% gold loading. For comparison, the results of bare iron oxide nanoparticles (without any gold) were included.

Figure 4 shows the magnetic-induced heating responses for nano-antenna susceptor aqueous samples. Data shows a rapid temperature increase from t = 0 sec until approximately t = 800 seconds. The temperature of the solution reached 50 ˚C in approximately 20 minutes for all nanoparticles. A higher magnetic field should result in a higher rate of change for each type of nanoparticle. A heating rate of approximatively 5 °C/min in the first 20 min. Once the temperature reached around 50 °C, the temperature increase was less significant with a rate of 1-2°C/min. The same trend was recorded on gold decorated iron oxide and bare iron oxide nanospheres. Citrate and cetyltrimethylammonium bromide functionalized nanosphere samples also follow the same temperature profile (data not included for clarity). While the presence of gold nanospheres on the surface of the iron oxide nanoparticle has no significant impact on the initial rate of temperature increase or the final temperature that the solution reaches, the amount of gold present on the iron oxide nanoparticles does affect the final temperature. The highest magnetic-induced heating response is recorded on the iron oxide susceptors decorated with the highest amount of gold nanomaterials (Figure 4). These results are in agreement with the EDS composition studies and specific loss power theoretical calculations. It is believed that the heat transfer between particles is more efficient when more gold is present on the iron oxide resulting in higher temperature profiles. The iron oxide-gold nanoparticles open the door to further investigate them for photothermal applications by transducing light to heat through plasmonic absorbance of gold.

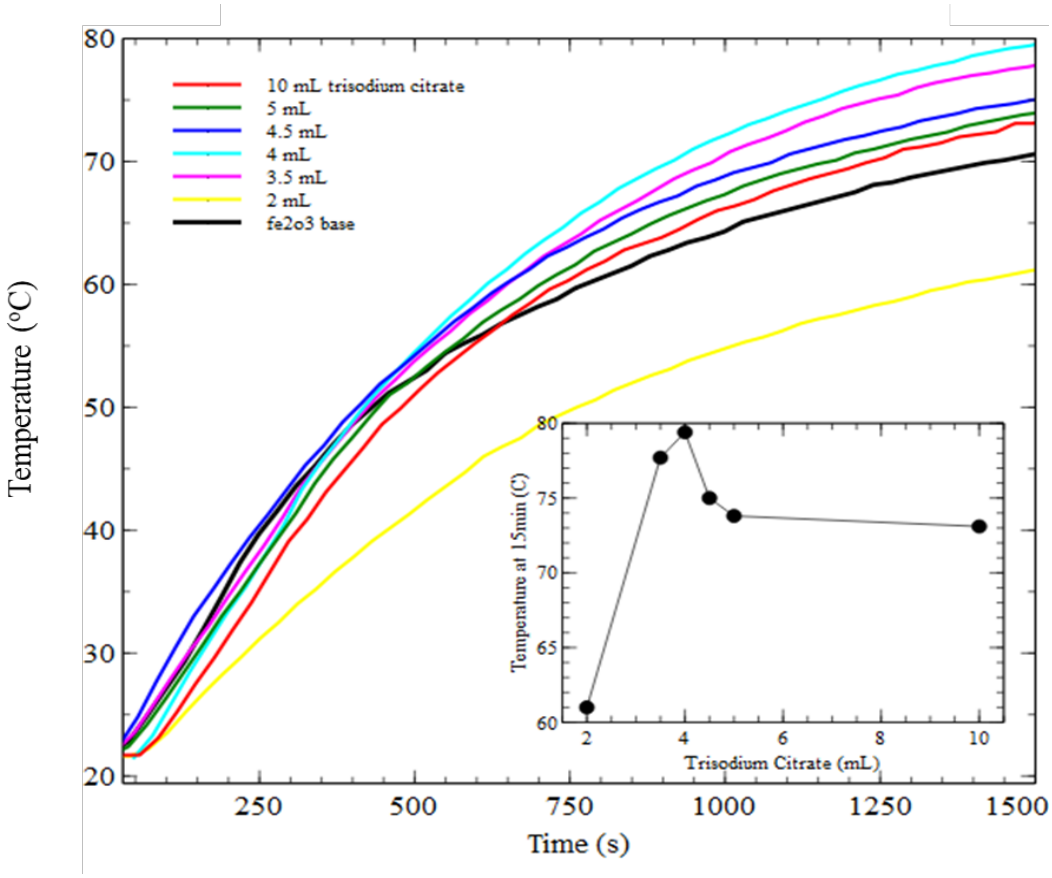

Figure 4. The temperature change of iron oxide-gold nano-antenna susceptor materials nanocomposites. Inset data shows the temperature dependence with the gold loading that is in agreement with the energy dispersive X-Ray spectroscopy data.

4.4. Adsorption and release of organic dyes

In this section, methylene blue (MB), a cationic organic dye, was used for the adsorption and desorption of from iron oxide nanoparticles as shown in figure 5. Desorption process was monitored and magnetically induced by applying energy to solutions containing methylene blue sorbed on iron oxide nanoparticles. The effect of surface ligands, including citrate and cetyltrimethylammonium bromide, on the adsorption was investigated. The nanostructures were incubated in ligands for several hours before exposure to the methylene blue. The sorption of methylene blue onto the nano-susceptors was measured by monitoring the absorbance of the methylene blue solution at 2 hours intervals. As shown in Figure 5, methylene blue did not adsorb onto unmodified (bare) iron oxide or cetyltrimethylammonium bromide functionalized iron oxide. However, the adsorption was successfully achieved on citrate capped iron oxide nanoparticles. Since the iron oxide-citrate particles had a more negative zeta potential and was the only sample to adsorb methylene blue, the adsorption is most likely a physisorption mechanism due to van der Waals attractions between the negatively charged citrate groups and the positively charged methylene blue. The weak interactions are also very sensitive to pH variations and solution ionic strength which could explain the differences in adsorption process.

Magnetic induced hyperthermia was used to release adsorbed materials from magnetic susceptor nanostructures. The adsorbed methylene blue was released from the iron oxide nanoparticles due to localized temperature increase on the nanomaterial and, subsequently, in the surrounding solutions. Magnetic hyperthermia studies led to a desorption efficiency around 19% after 30 minutes of magnetic heating at 85 ºC. Before heating, there was a small amount of methylene blue that desorbed under ultraviolet-visible exposure; however, a larger amount of methylene blue desorbed after exposure to a magnetic field (Figures 5 and 6).

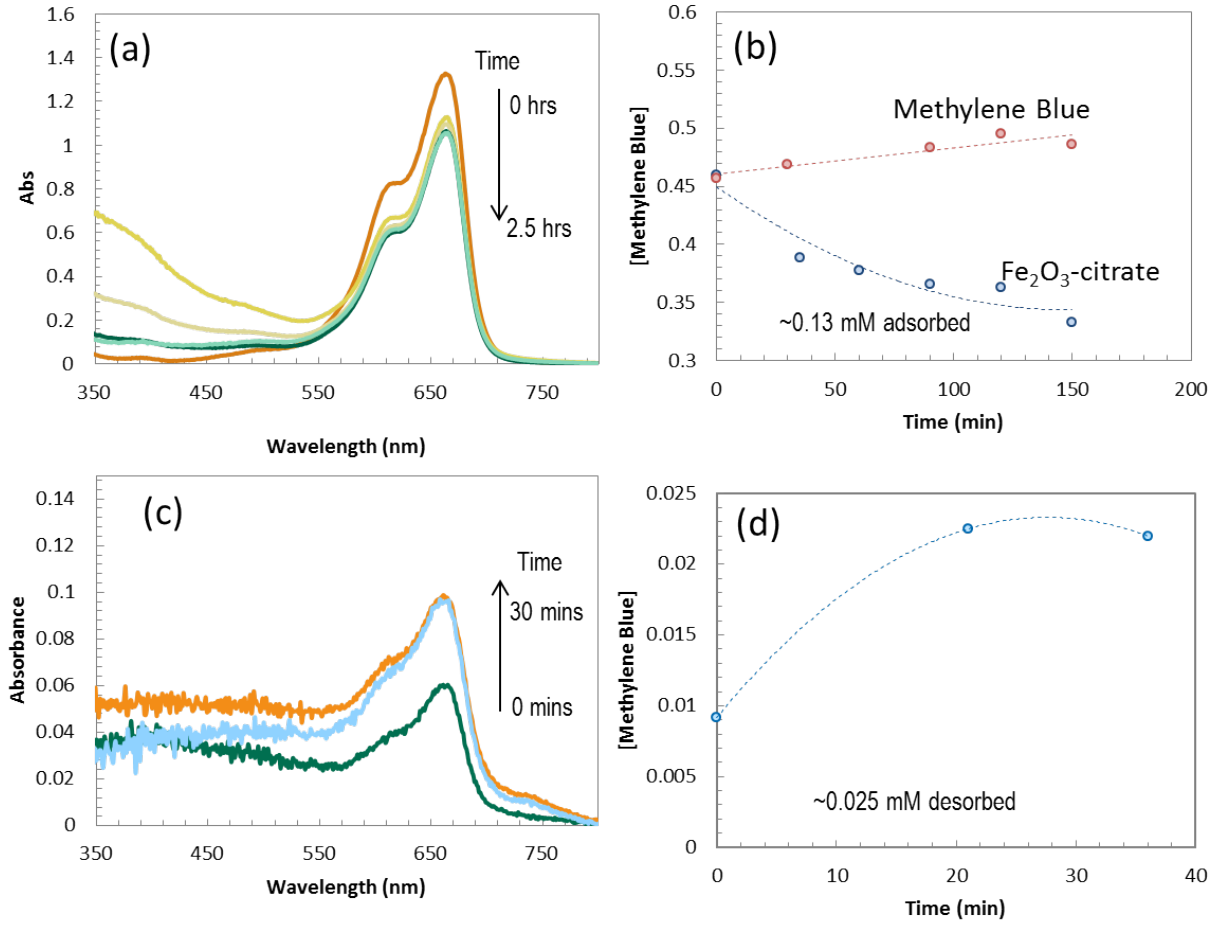

Figure 5. Absorption and desorption of iron oxide with methylene blue (a) Ultraviolet-visible during absorption; (b) change in concentration over time for methylene blue concentration adsorption; (c) Ultraviolet- visible of desorption; (d) change in methylene blue concentration over time for the desorption.

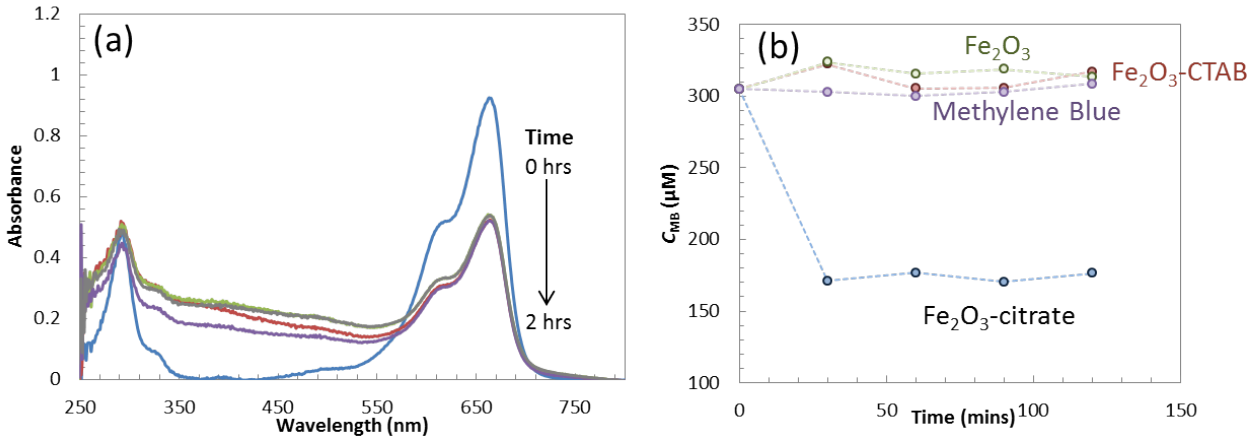

Figure 6. Adsorption of methylene blue (a) Ultraviolet-visible s for citrate over time and (b) scatter plots for iron oxide-citrate, iron oxide- cetyltrimethylammonium bromide and bare iron oxide nanoparticles.

5. Conclusions

This work demonstrates different approaches for surface engineering of iron oxide nanoparticles including: (a) a facile seed-mediated synthesis approaches to generate plasmonic-magnetic iron oxide-gold nanomaterials, and (b) one step surface functionalization with citrate and cetyltrimethylammonium bromide. It was found that trisodium citrate played a major role in the amount of gold loading produced onto iron oxide nanoparticles. A trisodium citrate concentration of 1.23 mMproduced the highest gold loading onto iron oxide nanospheres. Nanocomposites with higher gold loading percentages heated more efficiently during magnetic induction studies where temperature reached 78°C after 25 min. Citrate- and cetyltrimethylammonium bromide- capped iron oxide nanospheres were produced and investigated as efficient platforms for the extraction of organic dye contaminants. The technology was used to remotely remediate environments by scavenging and removing methylene blue from water sources. The ligand layer influenced methylene blue adsorption, which is evidence of an electrostatic adsorption. This system can be used for environmental remediation and recycling of the sorbed particles. The citrate capped iron oxide nanoparticles captured the organic dyes within several hours of incubation. Subsequently, the electromagnetic field was selectively coupled to engineered iron oxide-based nano-antenna susceptors for nanoparticle's regeneration and reuse. Remote manipulation of 'payloads' adsorbed on iron oxide-based materials was achieved through a non-contact and highly selective thermal process. Magnetic hyperthermia led to a desorption efficiency of methylene blue around 19% after 30 minutes of magnetic heating at 85°C. Contaminant dye removal via adsorption onto sorbent media is faster, easier, and more economic and is therefore viable for large scale implementation . These studies showed that iron-oxide nanoparticles can be used as efficient sorbent materials of contaminants due to their increased surface area-to-volume ratio and higher reactivity. Their surface chemistry can be easily tailored for targeted in situ sensing and remediation processes. It is envisioned that these novel nanostructures can be easily incorporated and used in industrial environmental remediation applications due to their low cost, magnetic recyclability, reusability and efficiency.

6. Acknowledgements

This work was supported by the Laboratory Directed Research and Development (LDRD) program within the Savannah River National Laboratory (SRNL). We would like to thank the Science Undergraduate Laboratory Internship (SULI) operated by the DOE-Office of Science and the Savannah River National Laboratory financial support. This work was produced by Battelle Savannah River Alliance, LLC under Contract No. 89303321CEM000080 with the U.S. Department of Energy. Publisher acknowledges the U.S. Government license to provide public access under the DOE Public Access Plan (http://energy.gov/downloads/doe-public-access-plan).

7. References

1. Hunyadi Murph SE, Lawrence K, Sessions H, Brown M, Larsen G (2020) Controlled Release of Hydrogen Isotopes from Hydride-Magnetic Nanomaterials, **ACS Applied Materials & Interfaces**, 12:9478-9488.

2. Kunz, PC.; Meyer, H; Barthel, J; Sollazzo, S.; Schmidt, AM.; Janiak, C, (2013) Metal carbonyls supported on iron oxide nanoparticles to trigger the CO-gas transmitter release by magnetic heating. **Chem. Commun**., 49, 4896-4898.

3. Hunyadi Murph SE, Searles, E (2021) Iron Oxide-Gold Composite Nanoparticles and Nano-Gap Junctions for Sensing Applications Using Surface -Enhanced Raman Scattering, in T.S. Srivatsan, W. Harrigan, Hunyadi Murph, S.E. (2021) Metal-Matrix Composites: Advances in Analysis, Measurement, and Observations, Springer Publisher, pp. 93-110.

4. Tao, CG; Cullen, WG; Williams, E.; Hunyadi, SE; Murphy, CJ (2007) Surface Morphology and Step Fluctuations on Silver Nanowires, **Surface Science**, 601:4939- 4943.

5. Hunyadi Murph SE, Jacobs S, Siegfried M, Hu T, Serkiz S, Hudson J. (2012) Manganese-Doped Gold Nanoparticles as Positive Contrast Agents for Magnetic Resonance Imaging (MRI). J. **Nanoparticle Res.,** 14:658-659.

6. Hunyadi Murph SE, Larsen G, Lascola R. (2016) Multifunctional Hybrid Fe2O3-Au Nanoparticles for Efficient Plasmonic Heating. **J. Visual Experiments** (JOVE), 108: e53598.

7. Lima-Tenório, MK; Gómez Pineda, EA; Ahmad, NM.; Fessi, H.; Elaissari, (2015) A. Magnetic Nanoparticles: In Vivo Cancer Diagnosis and Therapy. **Int. J. Pharm**., 493: 313−327.

8. Li D, Seaman J, Hunyadi Murph SE, Kaplan D, Taylor-Pashow T (2019) Porous iron material for TcO4- and ReO4- sequestration from groundwater under ambient oxic conditions**. Journal of Hazardous Materials**, 374: 177-185.

9. Srivatsan, TS, Harrigan, W, Hunyadi Murph, SE (2021) Metal-Matrix Composites: Advances in Analysis, Measurement, and Observations, Springer Publisher, 1-275.

10. Hunyadi Murph SE, Larsen G, Coopersmith K (2017) Anisotropic and shape-selective nanomaterials: structure-property relationships, nanostructure science and technology series. Springer Publisher, pp 1- 470.

11. Hunyadi Murph SE, Murphy CJ (2013) Patchy Silica-Coated Silver Nanowires as SERS Substrates. **J. Nanoparticle Res**. 15:1607.

12. Hunyadi Murph, SE, Turick, C, Thomas, D (2012) Metallic and Hybrid Nanostructures: Fundamentals and Applications", in Applications of Nanomaterials, 2012, Series ISBN: 1-62699-000-X, Vol.4: Nanomaterials and Nanostructures, Volume (4), J.N. Govil, ISBN: 1-62699-004-2, Studium Press LLC, USA.

13. Yang, MQ, Pan, X, Zhang, N, Xu, YJ (2013) A Facile One-Step Way to Anchor Noble Metal (Au, Ag, Pd) Nanoparticles on a Reduced Graphene Oxide Mat with Catalytic Activity for Selective Reduction of Nitroaromatic Compounds. **Cryst. Eng. Comm**, 15:6819−6828.

14. Schmidt, AM (2005) Induction heating of novel thermoresponsive ferrofluids. **J. Magn. Magn. Mater**., 289: 5-8.

15. Beecroft, LL, Ober, CK (1997) Nanocomposite Materials for Optical Applications. **Chem. Mater.**, 9: 302−1317.

16. Hunyadi Murph SE, Sessions H, Lawrence K, Brown M, Ward, P (2021) Efficient Thermal Processes using Alternating Electromagnetic Field for Methodical and Selective Release of Hydrogen Isotopes, **Energy and Fuels**, 35:3438-3448.

17. Talbot, D., Campos, JQ, Checa-Fernandez, BL et. al (2021) Adsorption of Organic Dyes on Magnetic Iron Oxide Nanoparticles. Part I: Mechanisms and Adsorption-Induced Nanoparticle Agglomeration **ACS Omega**, 6: 19086−19098.

18. Houas, A; Lachheb, H; Ksibi, M.; Elaloui, E.; Guillard, C.; Herrmann (2001) Photocatalytic degradation pathway of methylene blue in water, **J. Appl. Catal. B Environ**. 31: 145 – 157.

19. Panda, SJ, Aggarwal, I, Kumar, H, et al (2021), Magnetite nanoparticles as sorbents for dye removal: a review, **Environmental Chemistry Letters**, 19:2487–2525.

20. Keyhanian, F, Shariati, S, Faraji, M, Hesabi M (2016) Magnetite nanoparticles with surface modification for removal of methyl violet from aqueous solutions**, Arabian Journal of Chemistry,** 9: S348-S354.

21. Zhang, Z., Kong, J (2011) Novel magnetic Fe3O4@C nanoparticles as adsorbents for removal of organic dyes from aqueous solution **J. Hazardous Materials**, 193: 325-329.

22. Hunyadi Murph, SE; Serkiz, S; Fox, E; Colon-Mercado, H.; et al Synthesis, Functionalization, Characterization and Application of Controlled Shape Nanoparticles in Energy Production", Fluorine-Related Nanoscience with Energy Applications, ACS Symposium Series, Volume 1064, Chapter 8, 2011, 127-163.

23. Larsen, G.; Farr, W.; Hunyadi Murph, S.E. (2016) Multifunctional Fe2O3-Au Nanoparticles with Different Shapes: Enhanced Catalysis, Photothermal Effects, and Magnetic Recyclability", **J. Phys. Chem**. C, 120: 15162- 15172.

24. Hunyadi Murph SE, Sessions H, Lawrence K, Brown M, Ward, P (2021) Efficient Thermal Processes using Alternating Electromagnetic Field for Methodical and Selective Release of Hydrogen Isotopes, **Energy and Fuels**, 35: 3438-3448.